nzsee
NEW ZEALAND SOCIETY FOR EARTHQUAKE ENGINEERING

A risk-based framework to account for step-change behaviour in seismic assessment

F. Zaidi, A. Hulsey & K. J. Elwood
University of Auckland, Auckland, New Zealand.

ABSTRACT

In New Zealand, the seismic assessment of existing buildings focuses on life safety risk. The assessed capacity of a building is limited by the capacity corresponding to any vulnerability (or weakness) that can potentially lead to what the New Zealand Seismic Assessment Guidelines define as a "significant life safety hazard". Some weaknesses are specified by the guidelines as Severe Structural Weaknesses (SSWs), characterized by brittle or step-change behaviour, likely to result in catastrophic failure with severe consequences concerning life safety, and there is less confidence in assessing their capacities. Their capacities are considered conservatively by applying a factor of 2 to their assessed capacities. Further, for some other weaknesses, such as precast floors, that are not categorised as SSWs but may exhibit step-change behaviour, a factor of 2 is also currently recommended to account for the uncertainty in their capacity determination. However, these factors of 2 are arbitrary. This paper proposes a risk-based framework to rationalize such factors based on the following criteria: (1) equal probability of fatality at the probable capacity used for assessment and (2) equal Annual Individual Fatality Risk (AIFR). The framework quantifies the effect of the three characteristics of SSWs: brittle or step-change behaviour, large consequences, and less confidence compared to a benchmark component without such characteristics. The framework's application is demonstrated by considering the variation of each of the three characteristics for a range of assessed capacities and seismic hazard curves.

1 INTRODUCTION

New Zealand seismic assessment guidelines (MBIE et al., 2017) focus on assessment based on life safety considerations. The assessed capacity of a building is compared with the Ultimate Limit State (ULS) seismic demand, which is the design level demand for a similar new building according to NZS1170.5:2004 (Standards New Zealand 2004). The ratio of the assessed capacity to ULS seismic demand is reported as a percentage called %*NBS* score, i.e. % New Building Standard. A building rated at 100%*NBS* is expected to provide the minimum life safety performance expected of a similar new building. The minimum life safety

performance is defined as an acceptable life safety performance across all levels of shaking, which extends beyond the ULS level for a 100%*NBS* building. The assessment methodology has allowances built in to give confidence that a minimum life safety level is achieved at demands higher than X% ULS; however, the confidence reduces with increased demands (MBIE et al., 2017). The assessed capacity, thus, is not the collapse capacity of a building but rather a conservative capacity representative of a lower damage state.

A building rated at a %*NBS* lower than 100%, say X%, is expected to provide the same level of life safety at X% of ULS demand as a 100% *NBS* building at ULS (MBIE et al., 2017). Also, two buildings rated at the same X%*NBS* are expected to give the same life safety performance at X% ULS demand. Life safety performance may be quantified as the probability of fatality, which is the product of the probability of failure at X% ULS demand and the fatality rate. The fatality rate is the probability of a fatality given the failure of the building. Thus, if the fatality rates are expected to be the same for two buildings, the same probability of failure at X% ULS demand implies the same probability of fatality. Ideally, for the two buildings to provide equal life safety performance across all levels of demand, their life safety risk shall be the same. Life-safety risk can be quantified using Annual Individual Fatality Risk (AIFR), i.e. annual probability of an individual dying in a building during an earthquake. AIFR can be estimated by integrating over the full hazard curve and hence includes all possible levels of earthquake shaking, including beyond ULS. Hence, for comparison of any two buildings in terms of life safety performance, there may be two criteria to check for: (1) Equal probability of fatality at X% ULS demand and (2) Equal AIFR. Both conditions are not expected to be satisfied simultaneously. However, if the comparison is based on reference to a 'benchmark' case, all other cases may be required to have the probability of fatality at X% ULS demand and AIFR not higher than the benchmark case.

For some vulnerabilities identified during seismic assessment, which the NZ seismic assessment guidelines define as Severe Structural Weaknesses (SSWs), capacities are assessed more conservatively by applying a capacity-reduction factor of 2. According to the Guidelines, the characteristics of SSWs are that they exhibit brittle or step-change behaviour, likely to result in a catastrophic failure with severe consequences, and there is less confidence in the assessment of their capacity. Here a risk-based framework is proposed for quantifying/rationalizing this factor by equating components with and without SSW characteristics based on the two conditions discussed in the previous paragraph. These concepts can also be applied to other weaknesses that are not identified as SSWs, like the brittle failure modes of precast floor units, where the current guidelines increase the drift demand by a factor of 2.

2 COLLAPSE FRAGILITY AND AIFR

It is a well-established practice to define the probability distribution of a damage state (i.e. fragility curve) as a continuous function of some intensity measure (IM), e.g. spectral acceleration or peak ground acceleration, or an engineering demand parameter (EDP)., e.g. the peak inter-story drift ratio or the peak floor acceleration. Though different probability distributions are possible, lognormal distribution has been considered to be a reasonable distribution to define fragility curves and has been used extensively in past studies. (e.g. Kennedy et al., 1980, Ibarra and Krawinkler, 2005, Luco et al., 2007, Zareian and Krawinkler, 2007, Haselton et al., 2011, Liel et. al., 2011). A lognormal distribution is defined with a median capacity μ and variability β (logarithm of the standard deviation).

Given a fragility curve for a damage state, the mean annual frequency of reaching that damage state is determined by integrating the hazard curve at the building's location with the fragility curve using the risk integral approach (e.g. Luco et al., 2007). The risk integral (equation 1) gives the mean annual frequency of collapse (MAFC) if the fragility curve corresponds to a state of collapse. Figure 1 shows the calculation of MAFC. AIFR is obtained by multiplying the mean annual frequency of collapse with the consequence function (i.e. probability of fatality given collapse) as shown in equation 2 (Horspool et al., 2021).

$$MAFC = \int_0^{\infty} P(IM > im) \cdot \left| \frac{d(LS_{col})}{dIM} \right| dIM \quad (1)$$

where the first term inside the integral is the mean annual probability of exceedance (POE) of Intensity Measure represented by the hazard curve and the second term is the derivate of the fragility curve (or the probability density function). $P(F|LS_{col})$ is the fatality rate given collapse.

$$AIFR = MAFC \cdot P(F|LS_{col}) \quad (2)$$

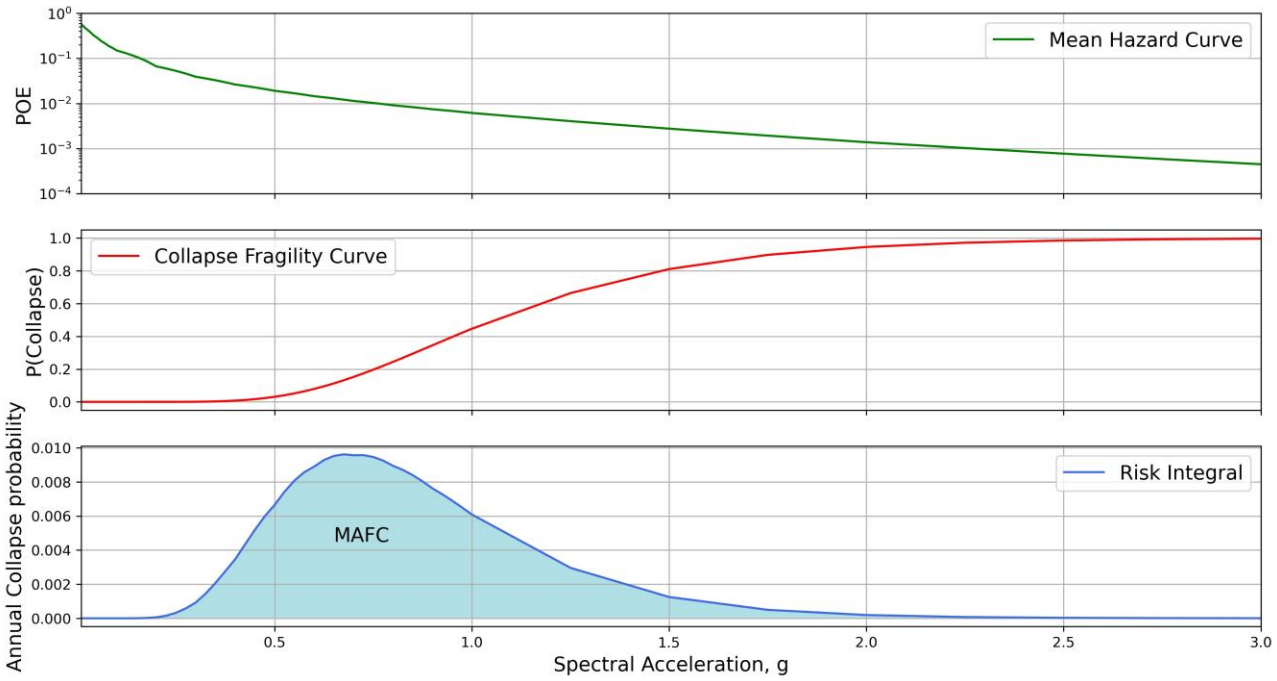

Figure 1: Calculation of Mean Annual Frequency of Collapse (MAFC)

2.1 Defining the hazard curve in terms of EDP

Fragility functions for components are generally defined in terms of an EDP, which is often the story drift ratio for drift-sensitive components. For working out MAFC, hazard information is required in terms of story drift ratio, or an EDP-IM relationship is required if the hazard information is in terms of IM, such as spectral acceleration.

An EDP-IM relationship can be developed for individual buildings by carrying out an Incremental Dynamic Analysis (Vamvatsikos and Cornell, 2002), multi-stripe analysis (Jalayer 2003), or techniques like SPO2IDA (Vamvatsikos and Cornell, 2006). A simplified form of an EDP-IM relationship can also be used with a median relationship and lognormal distribution (Cornell et al., 2002). With an EDP-IM relationship, the performance-based earthquake engineering (PBEE) framework (Deierlein et al., 2003) can be used to work out the annualized probability of exceeding a damage state or collapse for a specific component. Alternatively, we explore below a simpler approximate way using an EDP-IM relationship to specify the hazard curve in terms of the EDP critical for assessment.

If the fragility curves are in terms of story drift ratio (SDR), the mean hazard curve can be converted to be in terms of SDR using an SDR-IM relationship (e.g. Hulsey et al., 2022). Hulsey et al. considered critical SDR as the EDP which is the maximum SDR expected in a building. It is estimated as shown in equation 3.

$$SDR_{cr}(T) = \frac{C_{cr} Sd(T)}{h_e} \quad (3)$$

where $Sd(T)$ is the spectral displacement, h_e is the effective height of an equivalent single degree of freedom (SDOF) system, C_{cr} is the critical story factor to convert drift ratio of equivalent SDOF to SDR_{cr}. $Sd(T)$ is derived from $Sa(T)$ as

$$Sd(T) = Sa(T) \times \left(\frac{T}{2\pi}\right)^2 \quad (4)$$

This gives the $Sa - SDR_{cr}$ relationship as in equation 5.

$$Sa(T) = \left[\frac{h_e}{C_{cr}} \times \left(\frac{2\pi}{T}\right)^2\right] \times SDR_{cr}(T) = k(T) \times SDR_{cr}(T) \quad (5)$$

A simplified relationship between the peak critical story drift demand and spectral displacements has been employed for the assessment of older RC buildings exhibiting different mechanisms by FEMA P-2018 (FEMA 2018a). For example, for a 3-story RC moment frame building with period T_e = 0.5s and with a soft ground story, C_{cr} is estimated to be 2.28 with h_e = 8.4 m. Interested readers may refer to FEMA P-2018 for more details.

This simple relationship to link $Sa(T)$ to $SDR_{cr}(T)$ allows both the fragility curve and mean hazard curve to be defined in terms of normalized component capacity, which is linearly related to the spectral acceleration. Figure 2a shows the mean hazard curve for Wellington, $V_{s(30)}$ = 375m/s, T = 0.5s, based on the New Zealand National Seismic Hazard Model (NSHM) 2022 (GNS 2022).

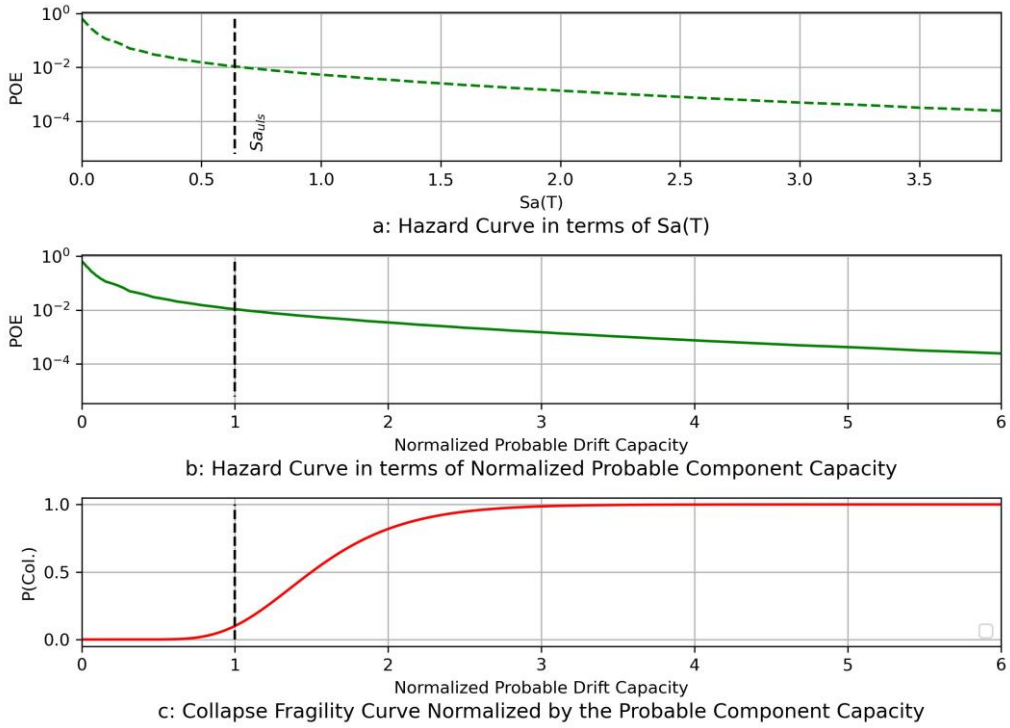

Figure 2: Hazard Curve in terms of Normalized Critical Story Drift Capacity for Wellington, $V_{s(30)}$ = 375m/s, T_e = 0.5s, 100%ULS - IL-2

If a building with T_e = 0.5s on a site with $V_{s(30)}$ = 375m/s in Wellington is rated to be at 100%*NBS* corresponding to the capacity of a component, both the hazard curve and the fragility curve of the component can be normalized based on the component's probable capacity. Figures 2b and 2c shows the normalized hazard and fragility curves. As described earlier, MAFC is calculated by integrating the hazard curve shown in Figure 2b with the fragility curves shown in Figure 2c.

3 COMPONENTS WITH SSW CHARACTERISTICS

Fragility curves for components are specified for different damage states in loss estimation frameworks (e.g. FEMA P-58 (FEMA 2018a)). Figure 3 shows the fragility curves for sequential damage states of a hypothetical component corresponding to three damage states of increasing severity: DS1, DS2, and DS3.

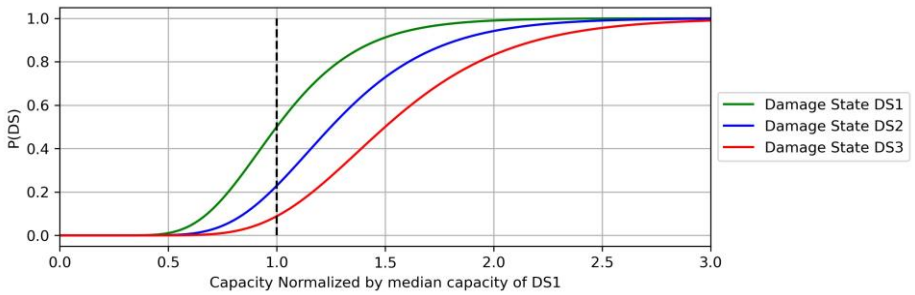

Figure 3: Sequential damage states (Adapted from FEMA P-58)

Suppose DS1 represents a state of damage consistent with the anticipated damage in a 100%ULS building for the ULS demand. In that case, the median of the fragility curve for DS1 represents the probable capacity of the component for assessment. If DS3 corresponds to a state of collapse, Figure 3 shows an example with a *buffer* of 1.5. Herein, we use the term *buffer* to refer to the margin between probable capacity and median collapse capacity. Also, the probable capacity corresponds to a small (around 10% in this example) probability of collapse on the collapse fragility curve (DS3). Hence, the probable capacity may alternatively be defined as the capacity corresponding to a specific probability of collapse at the collapse fragility curve.

Here, we differentiate components as either benchmark (BM) (i.e. without SSW characteristics) or as SSW components with one or more SSW characteristics (i.e. exhibit brittle or step-change behaviour, likely to result in a catastrophic failure with severe consequences, or there is less confidence in the assessment of their capacity). We look at these characteristics, one by one, and compare the BM and SSW components based on the adopted criteria of equal probability of fatality at the probable capacity, $P(Fat.)_{prob}$, and equal AIFR.

3.1 SSW1: components with step-change behaviour

Components with step-change behaviour exhibit a brittle, almost immediate degradation in response, i.e. they have minimal post-capping deformation capacity. They exhibit an abrupt increase in damage at the step change. This suggests that the fragilities for damage states DS1 to DS3 are closer together as depicted in Figure 4, compared to the typical (benchmark) case shown in Figure 3.

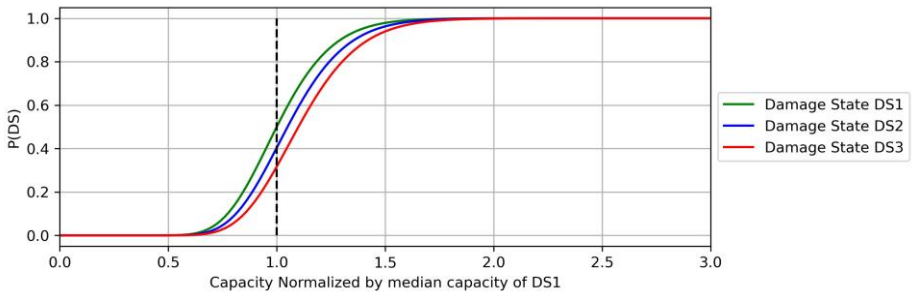

Figure 4: Sequential damage states for a component exhibiting step-change behaviour

Step change components may also be characterized by a steeper collapse fragility curve. Consider an extreme case of a stair supported on a ledge. If the seating is accurately measured for a particular stair, the fragility curve for the stair, defined in terms of movement at the ledge, is a step function. Also, since the component abruptly undergoes damage, the buffer to collapse is expected to be low if the probable capacity targets a particular state of damage and does not specifically account for the sudden change in behaviour expected at higher demands. Figure 5 shows both BM and SSW1 components having the same probability of collapse at the probable capacity, $P(Col.)_{prob}$. If the fatality rate for the two components is the same, equal $P(Col.)_{prob}$ means equal $P(Fat.)_{prob}$. Thus, the first criterion is met. However, an adjustment is required for the second criterion of equal AIFR.

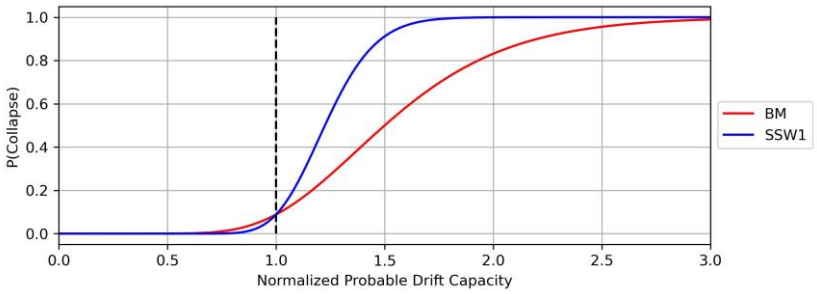

Figure 5: SSW1 component with step change behaviour

3.1.1 Adjustment for equal AIFR

Recall that AIFR is the product of the MAFC and the fatality rate. If the fatality rates for the two components are the same, the two components shall have the same MAFC. MAFC for the two components are calculated by integrating the respective fragility curves with the mean hazard curve as discussed in section 2. The fragility curve for the SSW1 component is shifted (green curve) such that its MAFC is equal to the MAFC of the BM component, as shown in Figure 6. The shift required is denoted as R_{AIFR}.

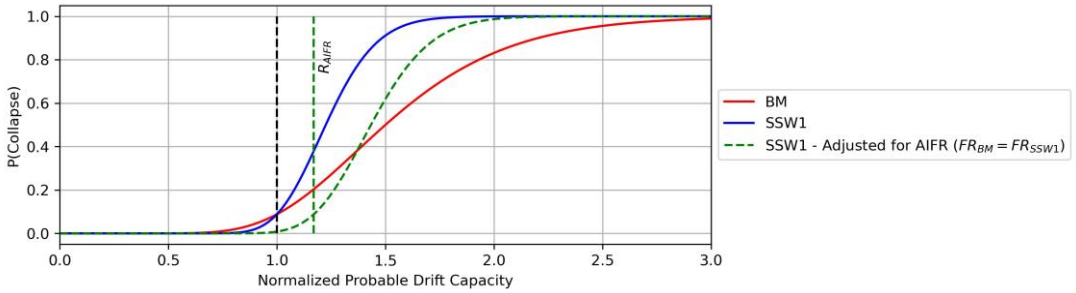

Figure 6: Adjustment for equal AIFR.

3.2 SSW2: components with higher uncertainty than the BM component

Uncertainty (or low confidence) in test results to represent actual in-situ behaviour introduces uncertainty in addition to the randomness in test results. For a component with lower confidence on account of a limited number of available test results or poor replication of in-situ conditions in test setup, such as precast floor units, a higher uncertainty is to be considered. Variability in capacity for this uncertainty, β_u, is suggested to be at least 0.25 as compared to a "usual" component uncertainty with β_u = 0.10 (FEMA 2018b). General randomness in test data differs for different mechanisms and the damage state for which the component is tested. However, for most cases, variability on account of test data dispersion, β_{td} is around 0.25-0.40

(FEMA 2018b). Figure 7 shows the collapse fragility for two components, both with $\beta_{td} = 0.3$ and a *buffer* of 1.5, but with different β_u ($\beta_u = 0.1$ for the BM component and $\beta_u = 0.25$ for the SSW2 component). The total variability is calculated using the square-root-of sum of squares (SRSS) method per FEMA P-58.

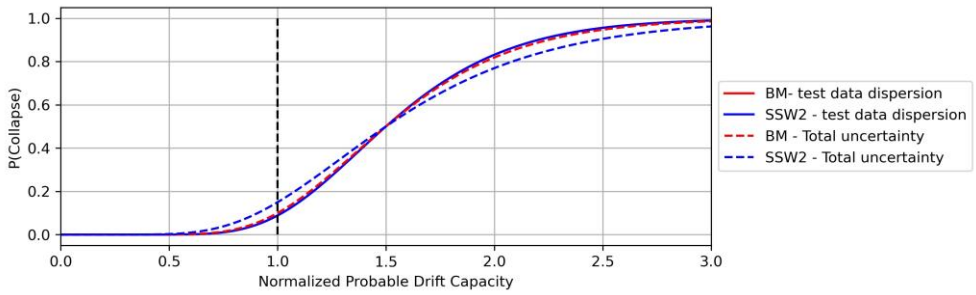

Figure 7: SSW2 component with higher uncertainty

Using the procedure discussed in section 3.1.1, for SSW2, the fragility only needs to be shifted slightly to achieve same AIFR as BM component. Figure 8 shows the shifted (green dashed) curve, such that the two components have the same MAFC (and AIFR), resulting in a shift of 1.03 times the probable capacity. The hazard curve shown in Figure 2b is used for calculation of MAFC.

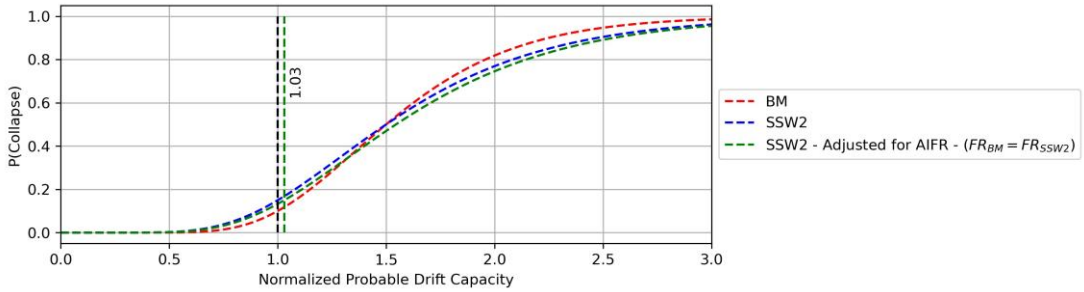

Figure 8: Adjustment for equal AIFR for SSW2. For Wellington, $V_{s(30)}$ = 375m/s, T_e = 0.5s, 100%ULS - IL-2

3.2.1 Adjustment for equal $P(Fat.)_{prob}$

In Figure 7, note that despite the same test data dispersion, because of the higher uncertainty in the capacity of the SSW2 component, $P(Col.)_{prob}$ of SSW2 is higher than that of the BM component. To have the same $P(Fat.)_{prob}$ as the BM component, an adjustment is required. Again, if the fatality rate for the two components is expected to be the same, the SSW2 (blue dashed) fragility curve requires shifting to the right till the SSW2 component has the same $P(Col.)_{prob}$ as the BM component. Figure 9 shows the shifted (green dashed) fragility curve. For this example, the shift required is 1.1 times the probable capacity. It is denoted here as $R_{P(Fat)}$.

Note that a *buffer* of 1.5 is considered here. However, if a larger *buffer* is considered, a lower $P(Col.)_{prob}$ is targeted. Because of the higher uncertainty in collapse fragility curve of the SSW2 component, $\beta_{u,SSW}$, there is a larger difference in capacities of the two components at the lower $P(Col.)_{prob}$. Thus, requiring a larger shift, as shown in Figure 10. Hence for *buffer* = 2, $R_{P(Fat)}$ is larger than for *buffer* = 1.5. This means, if a lower $P(Col.)_{prob}$ is desired for the components, the shift needs to be larger. In section 3.5, sensitivity of R to the two values of *buffer* is explored.

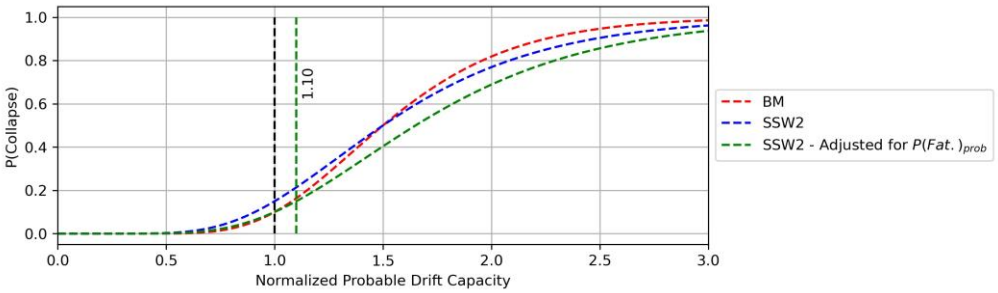

Figure 9: Adjustment for equal $P(Fat.)_{prob}$ for SSW2

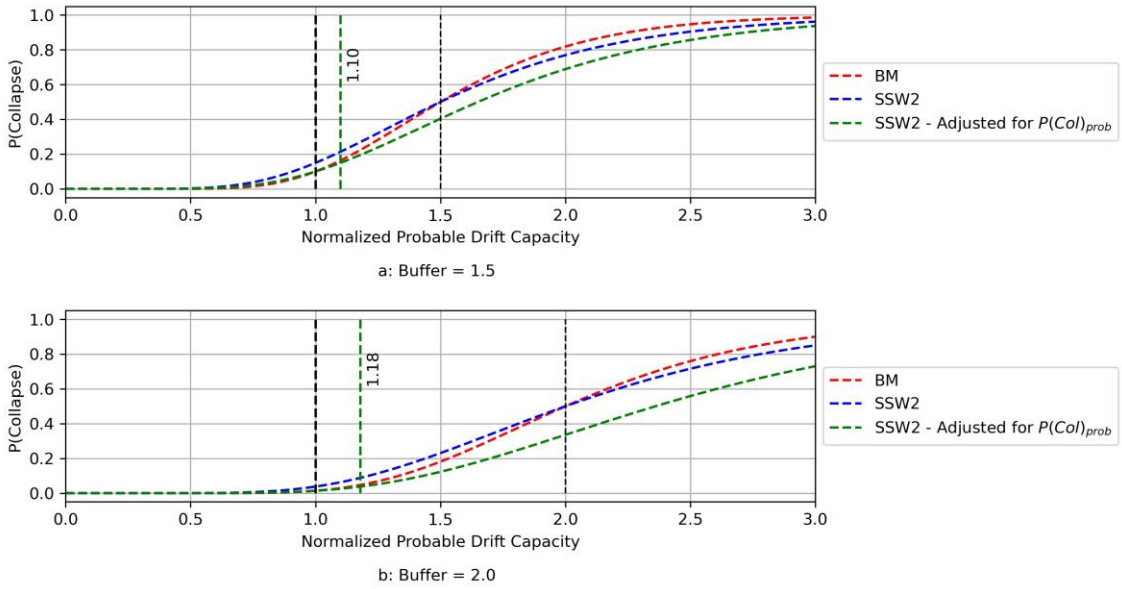

Figure 10: Effect of higher buffer on $R_{P(Fat)}$

3.3 SSW3: Components with higher consequence than the BM component

As discussed in section 2, consequence in this study is represented by the fatality rate given collapse. The fragility curve for BM and SSW3 components is the same, if the two components differ only in terms of consequences. However, considering a higher fatality rate for SSW3, adjustments are still required for the two criteria. To ensure SSW3 component has the same $P(Fat.)_{prob}$ and AIFR as the BM component, the fragility curve for SSW3 must be shifted to the right (i.e. higher capacity).

Figure 11 shows adjustment for $P(Fat.)_{prob}$. Considering that the fatality rate for SSW2 is twice that for the BM component, $P(Col.)_{prob}$ of SSW3 shall be half that of the BM component to have equal $P(Fat.)_{prob}$. $P(Col.)_{prob}$ of shifted green curve is half that of the BM component. The required shift here is 1.12.

Similarly, to have the same AIFR as the BM component, the fragility curve of SSW3 component requires shifting such that the MAFC for the SSW3 component is half that for the BM component. The shift required is shown in Figure 12. The hazard curve shown in Figure 2b is used for calculating R_{AIFR} in Figure 12.

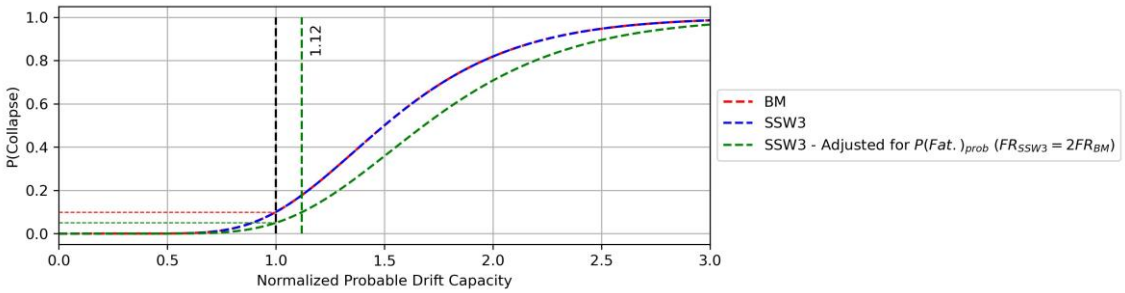

Figure 11: Adjustment for the equal $P(Fat.)_{prob}$ for SSW3 component with the same test data dispersion and uncertainty in test data to represent actual conditions, but twice the fatality rate as compared to the BM component. For Wellington, $V_{s(30)}$ = 375m/s, T_e = 0.5s, 100%ULS - IL-2

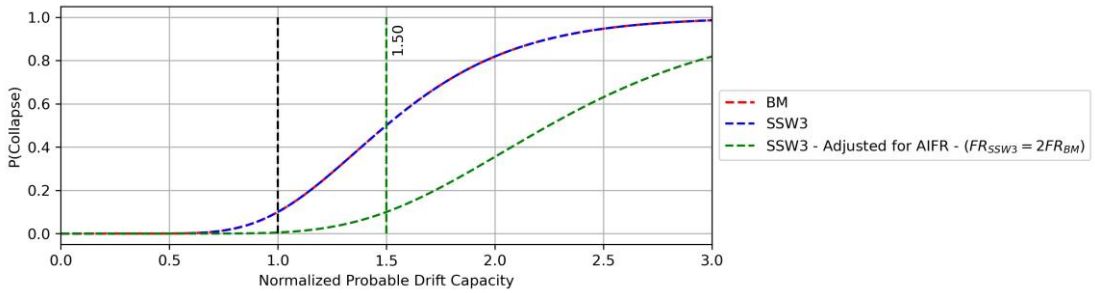

Figure 12: Adjustment for the equal AIFR for SSW3 component with the same test data dispersion and uncertainty in test data to represent actual conditions, but twice the fatality rate as compared to the BM component. For Wellington, Vs(30) = 375m/s, T_e = 0.5s, 100%ULS - IL-2

3.4 Combination of SSW characteristics

Figure 13 considers a component with SSW1 and SSW3 characteristics. The two green curves show adjustments for equal $P(Fat.)_{prob}$ and equal $AIFR$. Figure 14 shows adjustments for a component with SSW2 and SSW3 characteristics and Figure 15 shows the adjustments considering all three characteristics. The hazard curve shown in Figure 2b is used for calculating R_{AIFR} in Figures 13, 14 and 15.

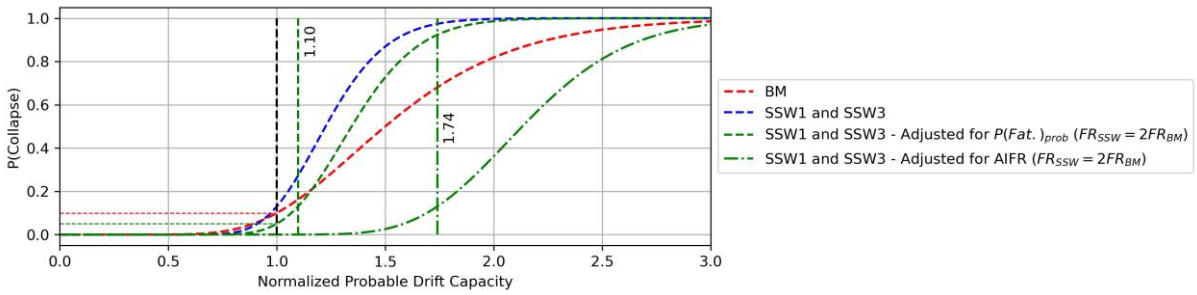

Figure 13: Adjustment for equal $P(Fat.)_{prob}$ and equal $AIFR$ for a component with SSW1 and SSW3 characteristics. For Wellington, $V_{s(30)}$ = 375m/s, T_e = 0.5s, 100%ULS - IL-2

($\beta_{td,BM} = 0.3$, $\beta_{td,SSW} = 0.15$, $\beta_{u,BM} = 0.1$, $\beta_{u,SSW} = 0.1$, $FR_{SSW} = 2FR_{BM}$)

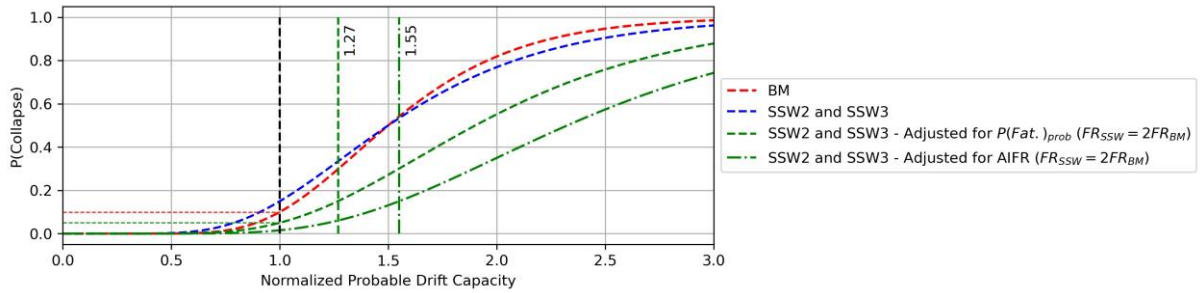

Figure 14: Adjustment for equal $P(Fat.)_{prob}$ and equal AIFR for a component with SSW2 and SSW3 characteristics. For Wellington, $V_{s(30)}$ = 375m/s, T_e = 0.5s, 100%ULS - IL-2

$(\beta_{td,BM} = 0.3,\ \beta_{td,SSW} = 0.3,\ \beta_{u,BM} = 0.1,\ \beta_{u,SSW} = 0.25,, FR_{SSW} = 2FR_{BM})$

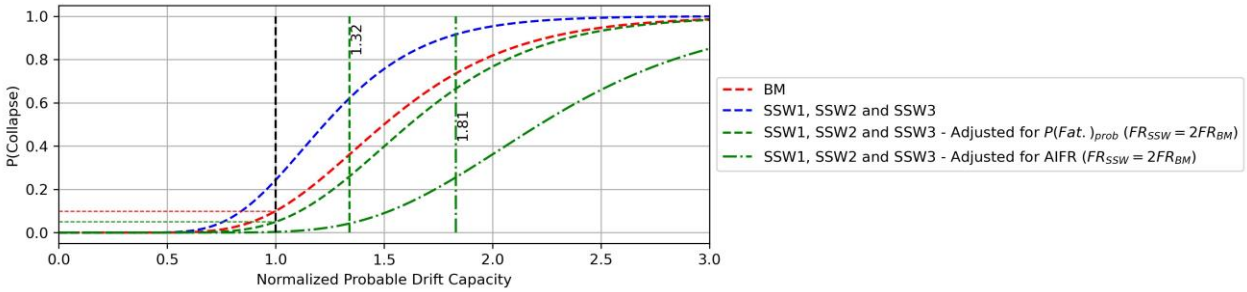

Figure 15: Adjustment for equal $P(Fat.)_{prob}$ and equal AIFR for a component with all three SSW characteristics. For Wellington, $V_{s(30)}$ = 375m/s, T_e = 0.5s, 100%ULS - IL-2

$(\beta_{td,BM} = 0.3,\ \beta_{td,SSW} = 0.15,\ \beta_{u,BM} = 0.1,\ \beta_{u,SSW} = 0.25, FR_{SSW} = 2FR_{BM})$

Recall from Figures 5 and 7 that to begin with the two components have the same $P(Col.)_{prob}$ based on respective β_{td}. However additional uncertainty β_u inflates the variability, thus resulting in a higher $P(Col.)_{prob}$. This effect is more pronounced for the component with all three SSW characteristics (blue curve in Figure 15) because it has a lower median capacity as compared to the BM component (red curve) to begin with due to lower $\beta_{td,SSW}$, and a higher uncertainty $\beta_{u,SSW}$ on top of it. Accordingly, the shifts required are the largest for the case with all three SSW characteristics.

Since R_{AIFR} is based on the integration with the mean hazard curve, it will not be the same for different towns, site categories, periods, or demand levels (%ULS). R_{AIFR} estimated across 12 New Zealand towns at different effective periods, site categories and demand levels are shown in Figure 16.

In Figure 16, it is observed that higher shifts are required for lower demand levels. This is due to generally flatter hazard curves (on a log scale) at a lower demand level, and hence, a larger shift is required to normalize for AIFR. A trend is also visible with increasing R_{AIFR} for larger periods and stiffer sites. This is also due to the relative shape of the hazard curve in the portion contributing most to the collapse risk. Figure 17a shows the hazard curve normalized at 100%ULS for different site categories for T = 0.5s for Wellington and Figure 17b shows the estimated R_{AIFR}. Note how a flatter hazard curve results in a larger shift.

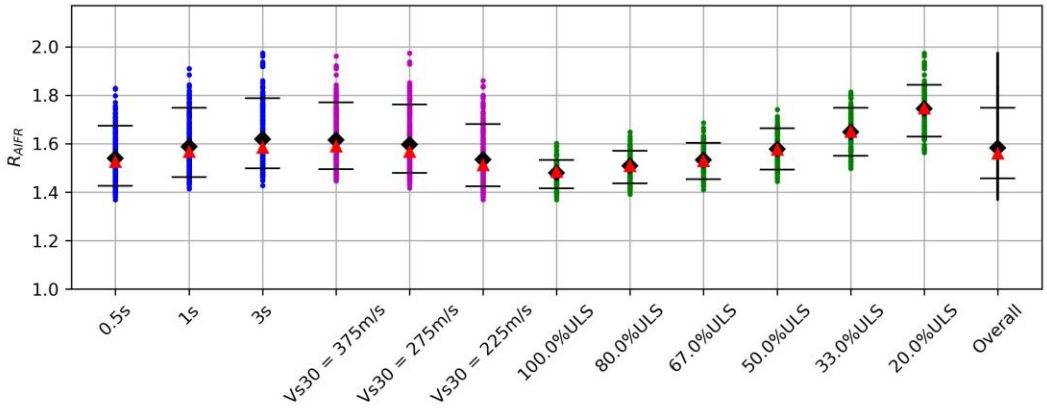

Figure 16: Adjustment for equal AIFR for a component with SSW2 and SSW3 characteristics

($\beta_{td,BM} = 0.3$, $\beta_{td,SSW} = 0.3$, $\beta_{u,BM} = 0.1$, $\beta_{u,SSW} = 0.25$, $FR_{SSW} = 2FR_{BM}$)

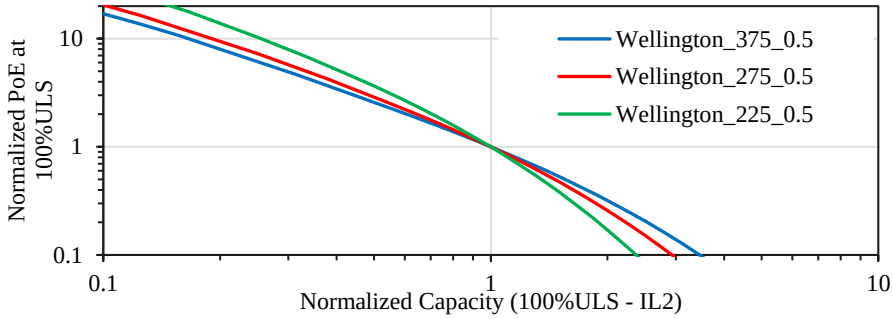

Figure 17a: Relative Shape of Hazard Curves for Wellington, $V_{S(30)}$ = 225m/s, 275 m/s, 375m/w, T = 0.5s

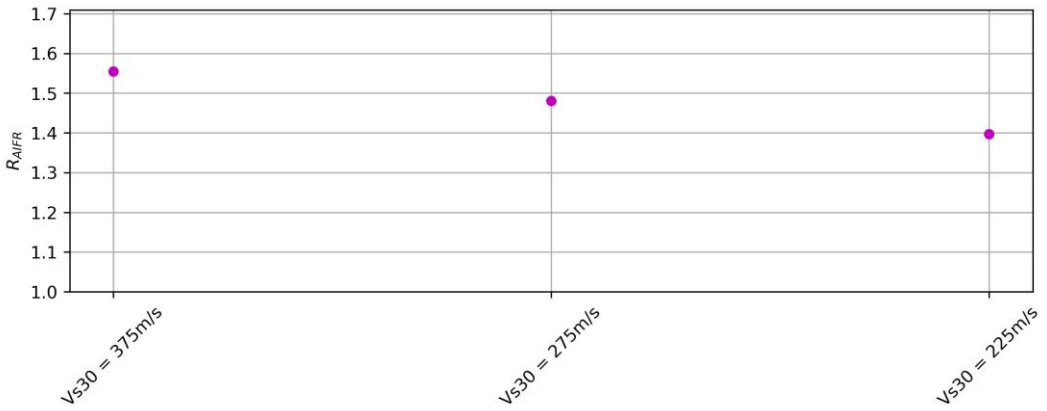

Figure 17b: Adjustment for equal AIFR for a component with the same test data dispersion as the benchmark component but higher uncertainty in test data to represent actual conditions for Wellington, $V_{S(30)}$ = 225m/s, 275 m/s, 375m/w, T = 0.5s

($\beta_{td,BM} = 0.3$, $\beta_{td,SSW} = 0.3$, $\beta_{u,BM} = 0.1$, $\beta_{u,SSW} = 0.25$, $FR_{SSW} = 2FR_{BM}$)

3.5 Sensitivity of R to β_{td}, β_u and FR

Since the adjustments are sensitive to the values assumed for β_{td}, β_u, FR, and *buffer* for the BM component, the adjustment factor R is estimated for a range of values as shown in Table 1. $\beta_{td,BM} = 0.3$ and

$\beta_{u,BM} = 0.1$ are kept constant. For the SSW component not to have the $P(Fat.)_{prob}$ and AIFR greater than the BM component, R is taken as the larger of $R_{P(Fat)}$ and R_{AIFR}. First three rows in Table 1 represent components not expected to exhibit step-change behaviour ($\beta_{td,BM} = \beta_{td,SSW}$) but have different uncertainties $\beta_{u,SSW}$ and fatality rates. The next six rows represent components with step-change (with different values of $\beta_{td,SSW}$) and with different uncertainties $\beta_{u,SSW}$ and fatality rates.

Note that larger adjustments are required for step change components with higher $\beta_{u,SSW}$. For higher $\beta_{u,SSW}$, $R_{P(Fat)}$ generally governs if the consequences are the same. However, if the consequences are large, R_{AIFR} is typically higher.

No change is observed in R_{AIFR} in the case of $\beta_{td,SSW}$ = 0.3 with the change in the *buffer* as the collapse capacity curves are the same irrespective of the *buffer* and thus require the same shift. However, in the case of lower $\beta_{td,SSW}$, with *buffer* =2, the collapse fragility curve is more to the left to begin with, thus requiring a larger shift to normalize for AIFR.

For high consequence cases, across the considered range of uncertainty and a *buffer* of 1.5 to 2.0 for the BM components, R_{AIFR} ranges from 1.5 to 2.2, generally consistent with SSW factor in the NZ Seismic Assessment Guidelines of 2.0.

Table 1: Sensitivity of $R_{P(Col)}$ and R_{AIFR} to assumed values of $\beta_{td,SSW}$, $\beta_{u,SSW}$, FR and buffer for the BM component (Values outside brackets are for buffer = 1.5 and those inside are for buffer = 2). Values of R_{AIFR} mentioned are the median values across different towns, site categories and demand levels.

$\boldsymbol{\beta_{td,SSW}}$	$\boldsymbol{\beta_{u,SSW}}$	$\boldsymbol{R_{P(Fat)}}$ $\boldsymbol{FR_{SSW} = FR_{BM}}$	$\boldsymbol{R_{P(Fat)}}$ $\boldsymbol{FR_{SSW} = 2FR_{BM}}$	$\boldsymbol{R_{AIFR}}$ $\boldsymbol{FR_{SSW} = FR_{BM}}$ ***median***	$\boldsymbol{R_{AIFR}}$ $\boldsymbol{FR_{SSW} = 2FR_{BM}}$ ***median***
0.3	0.1	1.00 (1.00)	1.12 (1.08)	1.00 (1.00)	1.50 (1.50)
0.3	0.25	1.10 (1.18)	1.26 (1.30)	1.04 (1.04)	1.56 (1.56)
0.3	0.4	1.25 (1.50)	1.51 (1.70)	1.10 (1.10)	1.68 (1.68)
0.2	0.1	1.02 (1.03)	1.10 (1.09)	1.10 (1.21)	1.65 (1.76)
0.2	0.25	1.15 (1.27)	1.29 (1.38)	1.15 (1.26)	1.72 (1.84)
0.2	0.4	1.35 (1.68)	1.59 (1.89)	1.22 (1.36)	1.85 (1.99)
0.15	0.1	1.03 (1.05)	1.10 (1.10)	1.17 (1.34)	1.74 (1.94)
0.15	0.25	1.19 (1.34)	1.32 (1.44)	1.21 (1.40)	1.81 (2.03)
0.15	0.4	1.41 (1.80)	1.64 (2.02)	1.29 (1.50)	1.95 (2.20)

Though not recognized as an SSW, for brittle failure modes of precast floor units the NZ seismic assessment guidelines suggest a factor of 2 to enhance the demand for their assessment considering high uncertainty in their probable capacity estimation. For precast hollow core slabs, the probable capacity of units is not the collapse capacity but corresponds to a 2 mm vertical drop of the panel observed in tests (Puranam et al.,

2021) suggesting availability of buffer that may be considered comparable with a benchmark component. It is further considered that the collapse of a precast floor unit will likely not lead to a higher consequence than most other components identified as significant life safety hazards and the test data dispersion is within the expected range for most components. Based on Table 1 for typical consequence levels and $\beta_{td,SSW}$ = 0.3, $R_{P(Fat.)}$ controls with values up to 1.5. Hence 1.5 may be a more reasonable estimate to increase the demand for assessment of precast floors.

Note that the starting premise considered here is that the BM and SSW components have the same $P(Col.)_{prob}$ based on test data dispersion. Generally, the probable capacities determined from the Assessment Guidelines may have different levels of conservatism built in. Thus, these factors are expected to vary compared to those estimated here. However, this framework provides an approach for normalizing the probable capacity of components based on the test data, confidence in the test data to represent actual behaviour and expected consequences.

4 CONCLUSION:

This paper has discussed a framework for normalizing probable capacity of components based on the three characteristics of SSWs: step-change behaviour, higher consequences, and low confidence in the probable capacity. The criteria used for normalization are equal probability of fatality at the probable capacity, implied by the same %*NBS* score, and equal AIFR, which is desired based on the life safety intent of the assessment. The framework is helpful in rationalizing the factors used for capacity reduction of SSWs and generally supports the factor of 2.0 included in the NZ Seismic Assessment Guidelines.

The framework is generic and can consider components that are not identified as SSWs, but have higher uncertainty like the precast floor units. Such components are not expected to pose higher consequences than most other components identified to pose a significant life hazard. A factor of around 1.5 may be a reasonable estimate for their assessment recognizing higher uncertainty in their capacity estimation.

5 REFERENCES

ASCE (2017). *"ASCE standard, ASCE/SEI, 41-17, Seismic evaluation and retrofit of existing buildings"*. American Society of Civil Engineers and Structural Engineering Institute, Reston, Virginia USA. https://doi.org/10.1061/9780784414859

Cornell CA, Jalayer F, Hamburger RO and Foutch DA (2002). "Probablistic Basis for 2000 SAC Federal Emergency Management Agency Steel Moment Frame Guidelines". *Journal of Structural Engineering*, **128**(4): 526-533. https://doi.org/10.1061/(ASCE)0733-9445(2002)128:4(526)

Deierlein GG, Krawinkler H and Cornell CA (2003). "A framework for performance based earthquake engineering". *7th Pacific Conference on Earthquake Engineering*, 13 – 15 Feburary, Christchurch, New Zealand, Paper No. 140. http://db.nzsee.org.nz/2003/View/Paper140s.pdf

FEMA (2009). "*FEMA P695. Quantification of building seismic performance factors"*. Federal Emergency Management Agency, USA. https://www.fema.gov/sites/default/files/2020-08/fema_earthquakes_quantification-of-building-seismic-performance-factors-component-equivalency-methodology-fema-p-795.pdf

FEMA (2018a). "*FEMA P-2018, Seismic Evaluation of Older Reinforced Concrete Buildings for Collapse Potential"*. Federal Emergency Management Agency, USA. https://www.fema.gov/sites/default/files/2020-08/fema_seismic-eval-older-concrete-buildings_p-2018.pdf

FEMA (2018b). "*FEMA P-58, Seismic Performance Assessment of Buildings: Volume 1- Methodlogy"*. Federal Emergency Management Agency, USA. https://femap58.atcouncil.org/

GNS (2022). *New Zealand National Seismsic hazard Model*. https://nshm.gns.cri.nz/ (Accessed 23 June 2023).

Haselton CB, Liel AB, Deierlein GG, Dean BS and Chou, J.H. (2011). "Seismic Collapse Safety of Reinforced Concrete Buildings. I: Assessment of Ductile Moment Frames". *Journal of Structural Engineering*, **137**(4): 481-491. https://doi.org/10.1061/(ASCE)ST.1943-541X.0000318

Horspool N, Gerstenberger MC and Elwood KJ (2021). "Risk targeted hazard spectra for seismic design in New Zealand". *NZSEE Annual Conference* 14-16 April, Christchurch, New Zealand, Paper No. 67. https://repo.nzsee.org.nz/bitstream/handle/nzsee/2324/Invited%20Horspool.pdf?sequence=1&isAllowed=y

Hulsey AM, Horspool N, Elwood KJ, Hooper JD and Gerstenberger MC (2022). "Risk targeted framework for seismsic design based on societal expectations of risk". *12th National Conference on Earthquake Engineering*, 27 June – 1 July, Salt Lake City, USA. https://eeri.org/what-we-offer/digital-library/?lid=12946

Ibarra FL and Krawinkler H (2005). "*Report No. 152 - Global Collapse of Frame Structures under Seismic Excitations*, Stanford University, Stanford, USA. https://stacks.stanford.edu/file/druid:dj885ym2486/TR152_Ibarra.pdf

Jalayer F (2003). "*Direct Probabilistic Seismic Analysis: Implementing Non-Linear Dynamic Assessments",* PhD Dissertation, Stanford University, Stanford, USA. https://www.researchgate.net/publication/234174752_Direct_Probabilistic_Seismic_Analysis_Implementing_Non-Linear_Dynamic_Assessments

Kennedy RP, Cornell CA, Campbell RD, Kaplan S and Perla HF (1980). "Probablistic Seismic Safety of a Nuclear Power Plant". *Nuclear Engineering and Design*, **59**(2): 315-338. https://doi.org/10.1016/0029-5493(80)90203-4

Liel AB, Haselton CB and Deierlein GG (2011). Seismic collapse safety of reinforced concrete buildings. II: Comparitive assessment of nonductile and ductile moment frames. *Journal of Structural Engineering*, **137**(4): 492-502. https://doi.org/10.1061/(ASCE)ST.1943-541X.0000275

Luco N, Ellingwood BR, Hamburger RO, Hooper JD, Kimball JK and Kircher CA (2007). Risk-Targeted versus Current Seismic Design Maps for the Conterminous United States. *SEAOC 2007 Convention Proceedings*. 26-29 September, Squaw Creek, USA, 163pp.

MBIE, NZSEE, SESOC, EQC and NZGS (2017). "*The Seismic Assessment of Existing Buildings – Technical Guidelines for Engineering Assessments*". Ministry of Business Innovation and Employment, New Zealand Society for Earthquake Engineering, Structural Engineering Society, Earthquake Commission, New Zealand Geotechnical Society, Wellington, New Zealand. http://www.eq-assess.org.nz

Puranam AY, Corney SR, Elwood KJ, Henry RS and Bull DK (2021). "Seismic Performance of Precast Hollow-Core Floors: Part 2—Assessment of Existing Buildings." *ACI Structural Journal*, **118**(5): 65-77.

Standards New Zealand (2004). "*NZS1170.5: Structural Design Actions. Part 5: Earthquake Actions - New Zealand*". Standards New Zealand, Wellington. https://www.standards.govt.nz/sponsored-standards/building-standards/NZS1170-5

Vamvatsikos D and Cornell CA (2002). "Incremental Dynamic Analysis". *Earthquake Engineering and Structural Dynamics*, **31**(3): 491-514. https://doi.org/10.1002/eqe.141

Vamvatsikos D and Cornell CA (2006). "Direct estimation of the seismic demand and capacity of oscillators with multi-linear static pushovers through IDA". *Earthquake Engineering and Structural Dynamics*, **35**(9): 1097-1117. https://doi.org/10.1002/eqe.573

Zareian F and Krawinkler H (2007). "Assessment of probability of collapse and design for collapse safety". *Earthquake Engineering and Structural Dynamics*, 36(13): 1901-1914. https://doi.org/10.1002/eqe.702